Editors' Suggestion

Light-Driven Electron-Hole Bardeen-Cooper-Schrieffer-Like State in Bulk GaAs

Yuta Murotani,[1] Changsu Kim,[2] Hidefumi Akiyama,[2] Loren N. Pfeiffer,[3] Ken W. West,[3] and Ryo Shimano[1,4]
[1]Department of Physics, The University of Tokyo, Tokyo 113-0033, Japan
[2]The Institute for Solid State Physics, The University of Tokyo, and OPERANDO-OIL, Kashiwa 277-8581, Japan
[3]Department of Electrical Engineering, Princeton University, Princeton, New Jersey 08544, USA
[4]Cryogenic Research Center, The University of Tokyo, Tokyo 113-0032, Japan

(Received 25 December 2018; revised manuscript received 1 July 2019; published 8 November 2019)

We investigate the photon-dressed state of excitons in bulk GaAs by optical pump-probe spectroscopy. We reveal that the high-energy branch of the dressed states continuously evolves into a singular enhancement at the absorption edge in the high-density region where the exciton picture is no longer valid. Comparing the experimental result with a simulation based on semiconductor Bloch equations, we show that the dressed state in such a high-density region is better viewed as a Bardeen-Cooper-Schrieffer-like state, which has been theoretically anticipated to exist over decades. Having seen that the dressed state can be regarded as a macroscopic coherent state driven by an external light field, we also discuss the decoherence from the dressed state to an incoherent state after the photoexcitation in view of the Coulomb enhancement in the transient absorption.

DOI: 10.1103/PhysRevLett.123.197401

Quantum condensation continues to be one of the most fascinating phenomena in condensed matter physics. The concept of a Cooper pair, which comprises two fermions and collectively condenses into a macroscopic quantum state to exhibit superfluidity, has led to great advances in the understanding of quantum many-body systems. After the original Bardeen-Cooper-Schrieffer (BCS) theory for superconductivity [1], many kinds of fermionic condensates where particles other than electrons form Cooper pairs have been unveiled. For example, fermionic helium atoms are paired to form a charge-neutral condensate in the superfluid ^{3}He [2]. BCS-type condensation has also been achieved rather recently in fermionic ultracold atomic gases [3,4].

An electron-hole (e-h) system in photoexcited semiconductors is another fascinating subject of pair condensation, which has raised a long-standing problem of BEC-BCS crossover [5–8]. In the low-density region, electrons and holes are strongly bound by Coulomb attraction to form quasibosonic elementary excitations, called excitons, which have been expected to undergo Bose-Einstein condensation (BEC) at sufficiently low temperatures [bottom of Fig. 1(a)]. On the other hand, in the high-density region where electrons and holes can form degenerate gases, a BCS-type condensation forming weakly bound e-h Cooper pairs has long been anticipated, where the coherence length exceeds the mean interparticle distance [top of Fig. 1(a)]. Such a quantum condensation is distinct from the formation of e-h liquid that usually takes the form of e-h droplets. In spite of numerous efforts dedicated so far, it still remains an open question how the exciton BEC and the e-h BCS state are connected to each other, due to the lack of systematic realization of condensed phases. Meanwhile, the idea of BEC-BCS crossover was successfully extended to different platforms of quantum condensation, such as ultracold atomic gases [9,10] and exciton-polariton systems [11,12]. Even recently it has gained renewed attention in the context of strong-coupling superconductivity in iron compounds [13,14] and excitonic insulators in narrow-gap semiconductors [15]. Stimulated by these active advances, elucidating the pioneering but unresolved e-h pair condensation in photoexcited semiconductors is strongly anticipated.

An advantage in e-h systems in direct-gap semiconductors is that the order parameter for pair condensation, i.e., the interband e-h polarization, can be directly induced by light with variable pair density or excitation intensity. As a result, a quasistationary condensate under monochromatic illumination [16,17] and a transient condensate after pulse excitation [18,19] have been theoretically predicted. Despite intensive theoretical studies over decades, this idea has been rarely addressed in experiments. Most experimental studies focused on a relatively low-density region where the results are interpreted in terms of the dressed states of excitons, which have been identified as optical Stark shift [20–23] and Autler-Townes splitting [24–28]. On the other hand, the high-density region where the concept of an exciton is replaced by a BCS-type pairing has remained unexplored. Because many-body interactions play an important role in the formation of an excitonic dressed state, its observation serves as a unique approach to study the highly correlated condensed phases in e-h systems, covering the whole BEC-BCS crossover region. In this sense, elucidating the behavior of dressed excitons

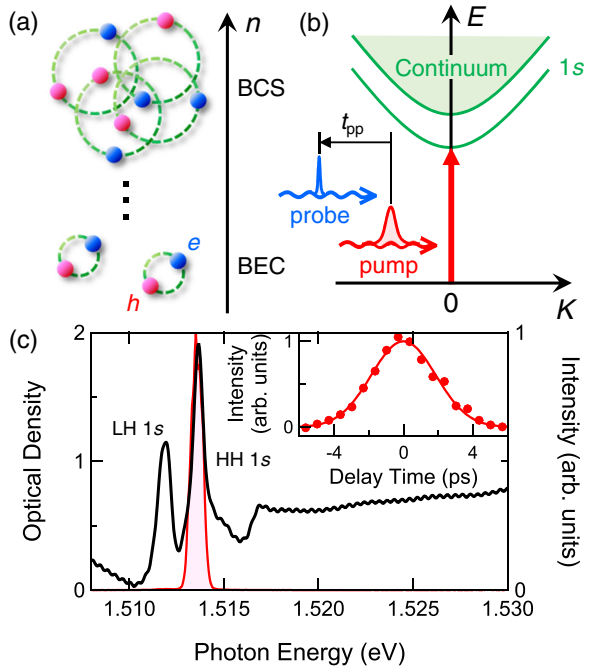

FIG. 1. (a) Conceptual diagram of BEC-BCS crossover in ultracold e-h systems. (b) Energy diagram of e-h pair excitations and schematic of the pump-probe measurement. (c) Optical density of the sample at 5 K (solid line) and intensity of the pump pulse (shaded curve). Inset: Autocorrelation signal of the pump pulse with a Gaussian fit.

under high-intensity illumination would pave the way for deeper understanding of condensed phases and for completing the global phase diagram of photoexcited semiconductors including the issue of exciton Mott transition (EMT) [29–37]. Motivated by this consideration, we investigated the dressed state of excitons in the high-density region by performing a pump-probe measurement on a direct-gap semiconductor, namely a bulk GaAs sample.

Figure 1(b) shows the schematic diagram of our experimental setup. We used a mode-locked regeneratively amplified Ti:sapphire laser system with 800 nm center wavelength and 30 fs pulse width as the light source. The laser output was divided into two beams for the intense pump and weak probe pulses. To coherently drive 1s excitons, the pump pulse was spectrally narrowed and tuned to the exciton resonance, as shown in Fig. 1(c) by the shaded curve. Correspondingly, the pulse duration is lengthened to 3.1 ps as estimated from the autocorrelation signal shown in the inset of Fig. 1(c). The pump pulse irradiated the sample with an incident angle of 10° and with a spot size of 0.4 mm after changing the intensity I with neutral density filters. The probe pulse was delayed by t_{pp} from the pump pulse by a translational stage and was incident normally on the sample with a spot size of 80 μm. We focused the transmitted probe pulse on a pinhole (a spatial filter) before detection and subtracted the scattered pump from the detected power spectrum. This procedure enabled us to calculate transient optical densities from the incident and transmitted power spectra of the probe pulse free from the pump scattering. The sample is a 1-μm-thick GaAs crystal grown by molecular beam epitaxy, sandwiched by 1.7-μm-thick $Al_{0.18}Ga_{0.82}As$ layers [37]. All the measurements were performed at 5 K using a ^{4}He-flow-type cryostat. Figure 1(c) shows the near-infrared optical density at 5 K exhibiting two sharp resonances corresponding to 1s states of light hole (LH) and heavy hole (HH) excitons. An in-plane tensile strain due to the lattice mismatch between GaAs and AlGaAs layers causes the LH-HH splitting. We concentrated on the HH 1s exciton resonance with the larger dipole moment to access the high-density regime with less pump intensity. The pump and probe beams were cocircularly polarized in order to exclude the biexciton effect [38]. Because we mainly focus on the temporal region where the pump pulse drives the interband coherence, we use the term "exciton" to indicate coherent excitons as long as incoherent excitons are not specified.

In Fig. 2(a), we show the transient optical density for various excitation intensities I at a fixed delay time $t_{pp} = 0$ ps. Along with I, a dimensionless parameter $r_s = (3/4\pi n)^{1/3} a_B^{-1}$ is indicated in the figure where $a_B = 14$ nm is the exciton Bohr radius and n is the e-h pair density estimated 50 ps after photoexcitation by the time-domain terahertz spectroscopy [37,39,40]. From $I = 0.06$ to 0.3 MW/cm^2, the HH exciton resonance splits into two peaks with increasing intensity. This behavior is distinct from the monotonic bleaching of the LH exciton resonance and clearly indicates the formation of the dressed state of HH excitons. It is discerned that the peak height of the

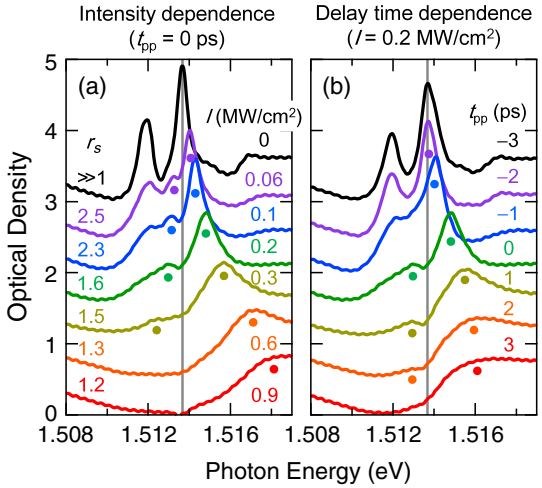

FIG. 2. Transient optical density measured (a) for various excitation intensities I at $t_{pp} = 0$ ps and (b) for various delay times t_{pp} at $I = 0.2$ MW/cm^2, both vertically shifted for clarity. Dots mark the split peaks of the HH exciton resonance. The pump photon energy is indicated by vertical lines. The dimensionless parameter r_s estimated 50 ps after photoexcitation is also indicated in (a).

higher-energy dressed state is always larger than the lower-energy one, which has been accounted for by the repulsive exciton-exciton interaction that pushes up the energy of excitons [27,28]. At $I \geq 0.6$ MW/cm^2, however, such a simple picture of interacting excitons breaks: the lower-energy peak vanishes while the higher-energy one remains, exhibiting an edgelike shape. In this high-density region, the dressed state is no longer viewed as a simple excitonic analog of the dressed state in two-level systems and should be dominated by many-body interactions.

For comparison, Fig. 2(b) shows delay time dependence of the transient optical density at a fixed intensity, $I = 0.2$ MW/cm^2. Again, we observe a splitting of the HH exciton resonance in the pump-probe overlap region ($0 \leq t_{\rm pp} \leq 2$ ps). The magnitude of splitting grows as the pump pulse illumination sets in. After the pump passes through the sample ($t_{\rm pp} = 3$ ps), the lower-energy peak vanishes while the higher-energy peak remains. These behaviors reflect time evolution of many-body coherence in the e-h system driven by the pump light field.

To understand the behavior of the dressed state in the high-density region, we performed a numerical simulation based on the semiconductor Bloch equations (SBEs) [18,19,21,22,25,26,41,42]. We neglect polaritonic effects because they are negligible under the present condition where the excited pair density exceeds 10^{15} cm^{-3} [43]. To be exact, the excited density is not homogeneous in the depth direction because of depletion of the pump pulse, which is neglected in the model (see Sec. I in Supplemental Material [44]). Therefore, we confine ourselves to a qualitative comparison between experiment and theory. We found that it is sufficient to consider the simplest model where only a constant dephasing of the interband e-h polarization $P_{\mathbf{k}}$ is taken into account to understand the experimental behavior. Details of the simulation are described in Sec. II in Supplemental Material [44].

Figure 3(a) shows the simulated absorption spectra $\mathrm{Im}[\chi(\omega)]$ for different peak electric fields E_0 of the pump pulse at $t_{\rm pp} = 0$ ps. Here, $\chi(\omega)$ is the electric susceptibility for a weak probe pulse, $\hbar\omega$ is the photon energy, E_g is the band gap energy, and E_b is the exciton binding energy. The spectrum of the pump pulse is also plotted at the top of the panel. When the sample is unexcited ($E_0 = 0$), the absorption spectrum shows a clear $1s$ exciton resonance below the edge of the high-energy continuum states. As the pump electric field is increased, the $1s$ exciton line splits into two, with the higher-energy peak exhibiting larger spectral weight than the lower-energy peak. At the highest excitation intensity shown in the panel ($E_0 = 0.05$), the higher-energy structure is heavily broadened so that it looks like an absorption edge rather than a peak. All these characteristics reproduce the experimental result reasonably well, assuring the validity of SBEs for the present problem.

Now, let us discuss the effect of many-body interactions on the dressed state of excitons based on the simulated

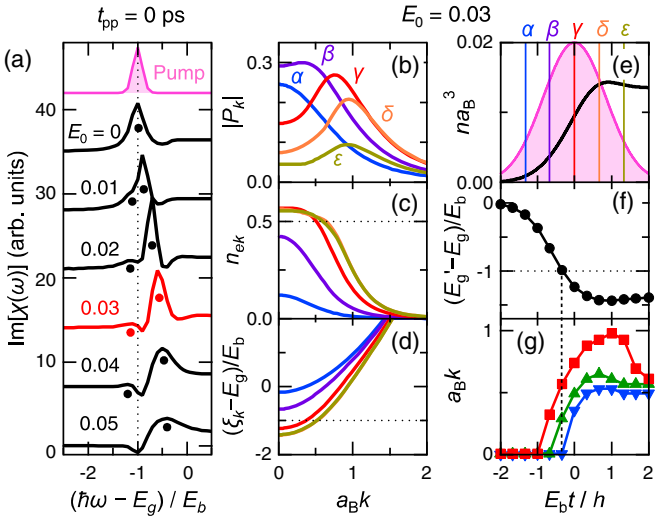

FIG. 3. Results of simulation. (a) Transient absorption spectra for different pump electric field E_0 at $t_{\rm pp} = 0$ ps, vertically shifted for clarity. Dots mark the split peaks. The pump spectrum is also shown on the top. (b)–(d) Snapshots of e-h polarization $|P_{\mathbf{k}}|$, electron density $n_{e\mathbf{k}}$, and renormalized pair energy $\xi_{\mathbf{k}}$, respectively, calculated for $E_0 = 0.03$ and labeled from α ($t < 0$) to ε ($t > 0$). (e) Time evolution of total pair density n (solid line) and pump intensity (shaded curve). Times corresponding to α–ε are also shown as vertical lines. (f) Dynamics of the renormalized band gap. (g) Time evolution of the peak position of $|P_{\mathbf{k}}|$ (squares), the quasi-Fermi wave number at which $n_{e\mathbf{k}} = 0.5$ (upward triangles), and resonantly excited wave number at which $\xi_{\mathbf{k}} = E_g - E_b$ (downward triangles). For the latter two, $k = 0$ indicates no solution.

results. For this purpose, we focus on the interband e-h polarization $P_{\mathbf{k}}$ induced by the pump electric field, which can be regarded as the wave function of coherent e-h pairs [42,53]. Figures 3(b)–3(d) show snapshots of $|P_{\mathbf{k}}|$, electron population $n_{e\mathbf{k}}$, and renormalized pair energy $\xi_{\mathbf{k}}$, respectively, from the early stage of photoexcitation (α) to the late stage (ε) for $E_0 = 0.03$. Figure 3(e) shows the corresponding times from left (α) to right (ε) along with the time-dependent pair density n and the pump intensity. Soon after the pump starts to excite the system (α), $|P_{\mathbf{k}}|$ is peaked at $k = 0$, displaying the wave function of the $1s$ exciton state. By contrast, at the maximum of the pump intensity (β, γ, and δ), $|P_{\mathbf{k}}|$ is peaked at a certain finite value of k, which is apparently distinguished from the ordinary exciton wave function at low densities. It is rather viewed as the wave function of an e-h Cooper pair, which peaks at the Fermi wave number [54,55]. Indeed, the electron population shown in Fig. 3(c) reaches half occupation (dashed line) at a wave number close to the peak position of $|P_{\mathbf{k}}|$. The appearance of the Cooper-pair-like wave function can be understood also in connection with EMT. The renormalized pair energy shown in Fig. 3(d) clearly shows the band gap renormalization (BGR), i.e., a global reduction, down to below the bare exciton energy (dashed line) in a small k

region. This is a simple but convenient criterion of EMT, because the charge-neutral excitons are less sensitive to surrounding carriers than unbound pairs [29]. In Fig. 3(f), we plot time evolution of the renormalized band gap $E_g' = \xi_{\mathbf{k}=0}$ along with the bare exciton energy (dashed line), depicting the transition from a low-density regime in which $E_g' > E_g - E_b$ to a high-density regime in which $E_g' < E_g - E_b$. In Fig. 3(g), we plot the time evolution of the characteristic wave numbers: the peak of $|P_{\mathbf{k}}|$ (squares), the quasi-Fermi wave number at which $n_{e\mathbf{k}} = 0.5$ (upward triangles), and the resonantly pumped wave number at which $\xi_{\mathbf{k}} = E_g - E_b$ (downward triangles). Note that $k = 0$ indicates no solution for the latter two. All these three quantities show a mutually correlated behavior; when all relaxation processes are neglected, it can be shown that the former two wave numbers exactly coincide. After the pump pulse passes through the sample (ε), the interband e-h polarization experiences the free-induction decay or dephasing, leaving an incoherent e-h population. From the above simulation, we deduce that the creation of Cooper-pair-like e-h pairs is specific to the high-density regime, where EMT occurs and quasi-Fermi surfaces are formed. This view can also be supported by the transient one-particle spectrum exhibiting a BCS-like gap structure inside the renormalized electron and hole continua: for further details, see Supplemental Material [44].

Finally, we address the so-called Coulomb enhancement (CE) effect. At low temperatures, the presence of Coulomb attraction between electrons and holes is known to enhance the gain and absorption near the quasichemical potential in photoexcited semiconductors, which is intensively studied with respect to the physics of semiconductor lasers [56–58]. To compare the pump-driven e-h BCS-like state and the CE effect, we plot in Fig. 4(a) the experimentally obtained transient optical density for $t_{\mathrm{pp}} = 3$, 10, and 100 ps by solid, dashed, and thin lines, respectively. At $t_{\mathrm{pp}} = 100$ ps, the peaklike or edgelike structures around 1.513 eV are identified as the Coulomb-enhanced absorption. By contrast, spectra at $t_{\mathrm{pp}} = 3$ ps show a distinct difference from those at $t_{\mathrm{pp}} = 100$ ps, where the higher-energy absorption is prominently enhanced and lower-energy weight is substantially suppressed. The high-energy hump structure develops continuously from the higher-energy peak of the dressed-state doublet. Therefore, we attribute the difference between the spectra at 3 ps and after 10 ps to the pump-induced coherence effect. At $t_{\mathrm{pp}} = 10$ ps, the spectra have already approached those at $t_{\mathrm{pp}} = 100$ ps, indicating the decoherence of the macroscopic polarization. To see it more clearly, we integrated the positive difference of the optical density from that at $t_{\mathrm{pp}} = 100$ ps as an indicator of coherence. The result is shown in Fig. 4(b) for $I = 0.06$ (triangles), 0.2 (squares), and 0.9 MW/cm^2 (circles). In all cases, the integrated signal decays within 10 ps. We approximate them with

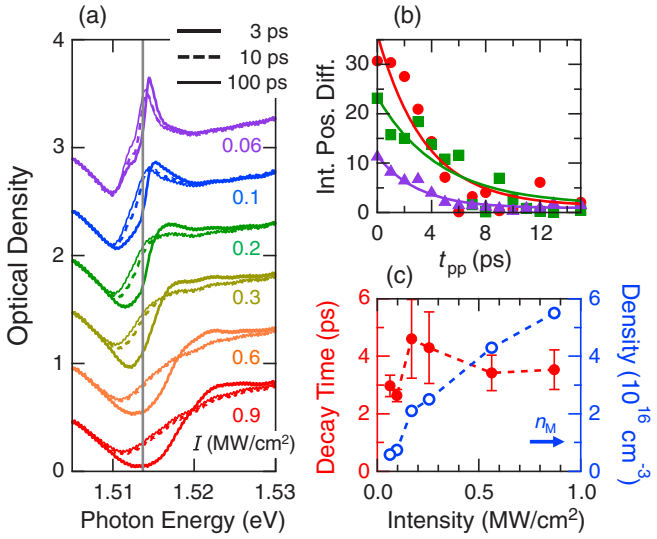

FIG. 4. (a) Transient optical density for $t_{\mathrm{pp}} = 3$ (solid lines), 10 (dashed lines), and 100 ps (thin lines), measured for different pump intensities I indicated. Spectra are vertically shifted for clarity. The pump photon energy is shown as a vertical line. (b) Integrated positive difference between optical density at $t_{\mathrm{pp}} \neq 100$ ps and that at $t_{\mathrm{pp}} = 100$ ps. Triangles, squares, and circles are for $I = 0.06$, 0.2, and 0.9 MW/cm^2, respectively. Lines are exponential fitting. (c) Intensity dependence of decay time of integrated positive difference (solid circles), and pair density measured at $t_{\mathrm{pp}} = 50$ ps (open circles).

exponential fits to obtain a measure of decoherence time, as shown by solid lines in the figure, though some of them show nonexponential decay because of the trailing edge of the pump pulse. The result is summarized in Fig. 4(c) as solid circles with fitting errors. In the same panel, the pair density measured 50 ps after the photoexcitation by terahertz spectroscopy is also plotted as open circles. Its value can be quantitatively compared with an experimental report on dynamical EMT in a similar sample observed by optical pump-terahertz probe spectroscopy [37]. Over a wide range of excited pair density across EMT with the Mott density $n_M \sim 1 \times 10^{16}$ cm^{-3} [37,59], the decay time remains 3–4 ps, comparable with the pump duration which drives the coherence of the system. Therefore, we conclude that the pump-induced coherence plays a crucial role in the transient optical density for $t_{\mathrm{pp}} \lesssim 3$ ps. The temporal evolution of the higher-energy dressed state indicates that the coherently driven macroscopic polarization state characterized by the BCS-like wave function continuously evolves into the Coulomb-enhanced band edge profiles after the decoherence time of about 3 ps.

In summary, we observed the photon-dressed states of 1s heavy hole excitons in a bulk GaAs by a pump-probe measurement. At low excitation intensity, the dressed states manifest themselves as an Autler-Townes doublet of the 1s exciton resonance. The higher-energy peak is larger than the lower-energy one, which is attributed to the blueshift of

the exciton resonance caused by repulsive exciton-exciton interaction. At high excitation intensity, the lower-energy peak vanishes while the higher-energy one remains though it is heavily broadened. This behavior reflects the fact that the system enters the high-density regime above the Mott density where many-body effects dominate the dressed states beyond the simple two-level analogs. According to a simulation by semiconductor Bloch equations, we showed that coherently driven *e-h* pairs in such a high-density region exhibit a Cooper-pair-like wave function, peaked at a finite relative momentum k. This result indicates that the *e-h* BCS-like coherent state, where the interband polarization plays the role of an order parameter, is realized as a continuous crossover from excitonic dressed states. We also discussed a continuous transition from the coherent macroscopic polarization state related to the dressed states to an incoherent state related to Coulomb enhancement after the photoexcitation. This observation suggests a good agreement with a theoretical prediction that Coulomb enhancement can be regarded as a precursor of *e-h* condensation [31]. Direct observation of the interband polarization by correlation measurements and of the BCS gap structure by angle-resolved photoemission spectroscopy will enable a more detailed understanding of time evolution of the light-induced condensed states, which we leave as a future work.

We acknowledge M. Takayama for his assistance in the pump-probe experiments. We also thank Professor K. Asano for fruitful discussions. The work at The University of Tokyo is supported by JSPS Kakenhi (Grant No. JP15H02102). The work at Princeton University is funded by the Gordon and Betty Moore Foundation through the EPiQS initiative Grant No. GBMF4420, and by the National Science Foundation MRSEC Grant No. DMR-1420541. Y. M. is supported by JSPS Research Fellowship for Young Scientists.

[1] J. Bardeen, L. N. Cooper, and J. R. Schrieffer, Phys. Rev. **108**, 1175 (1957).
[2] E. R. Dobbs, *Helium Three* (Oxford University Press, New York, 2000).
[3] C. A. Regal, M. Greiner, and D. S. Jin, Phys. Rev. Lett. **92**, 040403 (2004).
[4] M. W. Zwierlein, C. A. Stan, C. H. Schunck, S. M. F. Raupach, A. J. Kerman, and W. Ketterle, Phys. Rev. Lett. **92**, 120403 (2004).
[5] L. V. Keldysh and Yu. V. Kopaev, Fiz. Tverd. Tela **6**, 2791 (1964) [Sov. Phys. Solid State **6**, 2219 (1965)].
[6] D. Jérome, T. M. Rice, and W. Kohn, Phys. Rev. **158**, 462 (1967).
[7] C. Comte and P. Nozières, J. Phys. **43**, 1069 (1982).
[8] P. Nozières and S. Schmitt-Rink, J. Low Temp. Phys. **59**, 195 (1985).
[9] S. Giorgini, L. P. Pitaevskii, and S. Stringari, Rev. Mod. Phys. **80**, 1215 (2008).
[10] M. Randeria, Nat. Phys. **6**, 561 (2010).
[11] M. Yamaguchi, K. Kamide, R. Nii, T. Ogawa, and Y. Yamamoto, Phys. Rev. Lett. **111**, 026404 (2013).
[12] R. Hanai, P. B. Littlewood, and Y. Ohashi, J. Low Temp. Phys. **183**, 127 (2016).
[13] Y. Lubashevsky, E. Lahoud, K. Chashka, D. Podolsky, and A. Kanigel, Nat. Phys. **8**, 309 (2012).
[14] K. Okazaki, Y. Ito, Y. Ota, Y. Kotani, T. Shimojima, T. Kiss, S. Watanabe, C.-T. Chen, S. Niitaka, T. Hanaguri, H. Takagi, A. Chainani, and S. Shin, Sci. Rep. **4**, 4109 (2014).
[15] Y. F. Lu, H. Kono, T. I. Larkin, A. W. Rost, T. Takayama, A. V. Boris, B. Keimer, and H. Takagi, Nat. Commun. **8**, 14408 (2017).
[16] C. Comte and G. Mahler, Phys. Rev. B **34**, 7164 (1986).
[17] C. Comte and G. Mahler, Phys. Rev. B **38**, 10517 (1988).
[18] T. Östreich and K. Schönhammer, Z. Phys. B **91**, 189 (1993).
[19] K. Hannewald, S. Glutsch, and F. Bechstedt, J. Phys. Condens. Matter **13**, 275 (2001).
[20] A. Mysyrowicz, D. Hulin, A. Antonetti, A. Migus, W. T. Masselink, and H. Morkoç, Phys. Rev. Lett. **56**, 2748 (1986).
[21] S. Schmitt-Rink and D. S. Chemla, Phys. Rev. Lett. **57**, 2752 (1986).
[22] S. Schmitt-Rink, D. S. Chemla, and H. Haug, Phys. Rev. B **37**, 941 (1988).
[23] M. Combescot and R. Combescot, Phys. Rev. Lett. **61**, 117 (1988).
[24] R. Shimano and M. Kuwata-Gonokami, Phys. Rev. Lett. **72**, 530 (1994).
[25] C. Ciuti, C. Piermarocchi, V. Savona, P. E. Selbmann, P. Schwendimann, and A. Quattropani, Phys. Rev. Lett. **84**, 1752 (2000).
[26] M. Saba, F. Quochi, C. Ciuti, D. Martin, J.-L. Staehli, B. Deveaud, A. Mura, and G. Bongiovanni, Phys. Rev. B **62**, R16322 (2000).
[27] M. Phillips and H. Wang, Phys. Rev. Lett. **89**, 186401 (2002).
[28] M. C. Phillips and H. Wang, Phys. Rev. B **69**, 115337 (2004).
[29] R. Zimmermann, K. Kilimann, W. D. Kraeft, D. Kremp, and G. Röpke, Phys. Status Solidi B **90**, 175 (1978).
[30] G. W. Fehrenbach, W. Schäfer, J. Treusch, and R. G. Ulbrich, Phys. Rev. Lett. **49**, 1281 (1982).
[31] R. Zimmermann and H. Stolz, Phys. Status Solidi B **131**, 151 (1985).
[32] D. W. Snoke and J. D. Crawford, Phys. Rev. E **52**, 5796 (1995).
[33] S. W. Koch, W. Hoyer, M. Kira, and V. S. Filinov, Phys. Status Solidi B **238**, 404 (2003).
[34] D. Semkat, F. Richter, D. Kremp, G. Manzke, W.-D. Kraeft, and K. Henneberger, Phys. Rev. B **80**, 155201 (2009).
[35] T. Suzuki and R. Shimano, Phys. Rev. Lett. **109**, 046402 (2012).
[36] F. Sekiguchi and R. Shimano, Phys. Rev. B **91**, 155202 (2015).
[37] F. Sekiguchi, T. Mochizuki, C. Kim, H. Akiyama, L. N. Pfeiffer, K. W. West, and R. Shimano, Phys. Rev. Lett. **118**, 067401 (2017).
[38] C. Sieh, T. Meier, F. Jahnke, A. Knorr, S. W. Koch, P. Brick, M. Hübner, C. Ell, J. Prineas, G. Khitrova, and H. M. Gibbs, Phys. Rev. Lett. **82**, 3112 (1999).
[39] R. Huber, F. Tauser, A. Brodschelm, M. Bichler, G. Abstreiter, and A. Leitenstorfer, Nature (London) **414**, 286 (2001).

[40] R. A. Kaindl, M. A. Carnahan, D. Hägele, R. Lövenich, and D. S. Chemla, Nature (London) **423**, 734 (2003).
[41] H. Haug and S. W. Koch, *Quantum Theory of the Optical and Electronic Properties of Semiconductors, 5th ed.* (World Scientific, Singapore, 2009).
[42] M. Kira and S. W. Koch, Prog. Quantum Electron. **30**, 155 (2006).
[43] A. C. Schaefer and D. G. Steel, Phys. Rev. Lett. **79**, 4870 (1997).
[44] See Supplemental Material at http://link.aps.org/supplemental/10.1103/PhysRevLett.123.197401, which includes Refs. [45–52], for homogeneity of photoexcitation, details of the simulation, and analysis of the transient one-particle spectrum.
[45] Y. Murotani, M. Takayama, F. Sekiguchi, C. Kim, H. Akiayama, and R. Shimano, J. Phys. D **51**, 114001 (2018).
[46] V. M. Galitskii, S. P. Goreslavskii, and V. F. Elesin, Zh. Eksp. Teor. Fiz. **57**, 207 (1969) [Sov. Phys. JETP **30**, 117 (1970)].
[47] L. V. Keldysh, Phys. Status Solidi B **188**, 11 (1995).
[48] S. Adachi, *GaAs and Related Materials: Bulk Semiconducting and Superlattice Properties* (World Scientific, Singapore, 1994).
[49] M. Kozhevnikov, B. M. Ashkinadze, E. Cohen, and A. Ron, Phys. Rev. B **52**, 17165 (1995).
[50] T. Yoshioka and K. Asano, Phys. Rev. B **86**, 115314 (2012).
[51] K. Asano and T. Yoshioka, J. Phys. Soc. Jpn. **83**, 084702 (2014).
[52] F. Bechstedt and S. Glutsch, Phys. Rev. B **44**, 3638 (1991).
[53] H. Haug and S. Schmitt-Rink, Prog. Quantum Electron. **9**, 3 (1984).
[54] T. Iida, Y. Hasegawa, H. Higashimura, and M. Aihara, Phys. Rev. B **47**, 9328 (1993).
[55] T. J. Inagaki and M. Aihara, Phys. Rev. B **65**, 205204 (2002).
[56] R. Zimmermann, Phys. Status Solidi B **86**, K63 (1978).
[57] H. Haug and D. B. T. Thoai, Phys. Status Solidi B **98**, 581 (1980).
[58] C. Ell, H. Haug, and S. W. Koch, Opt. Lett. **14**, 356 (1989).
[59] P. P. Edwards and M. J. Sienko, Phys. Rev. B **17**, 2575 (1978).